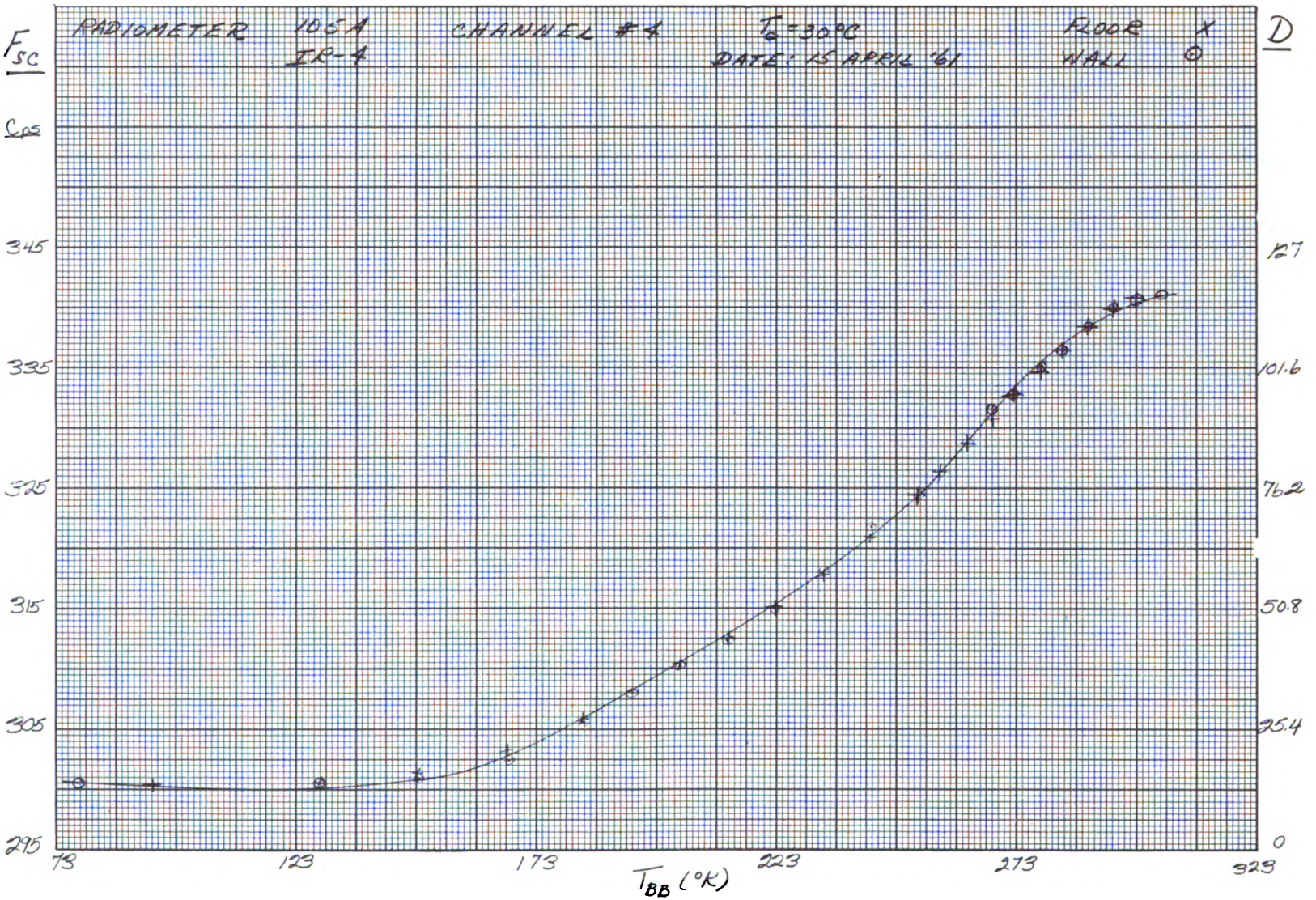

Figure 40—Subcarrier frequency and digital number vs. blackbody temperature for wall and floor sides, Channel 4. (T_c = 30°C)

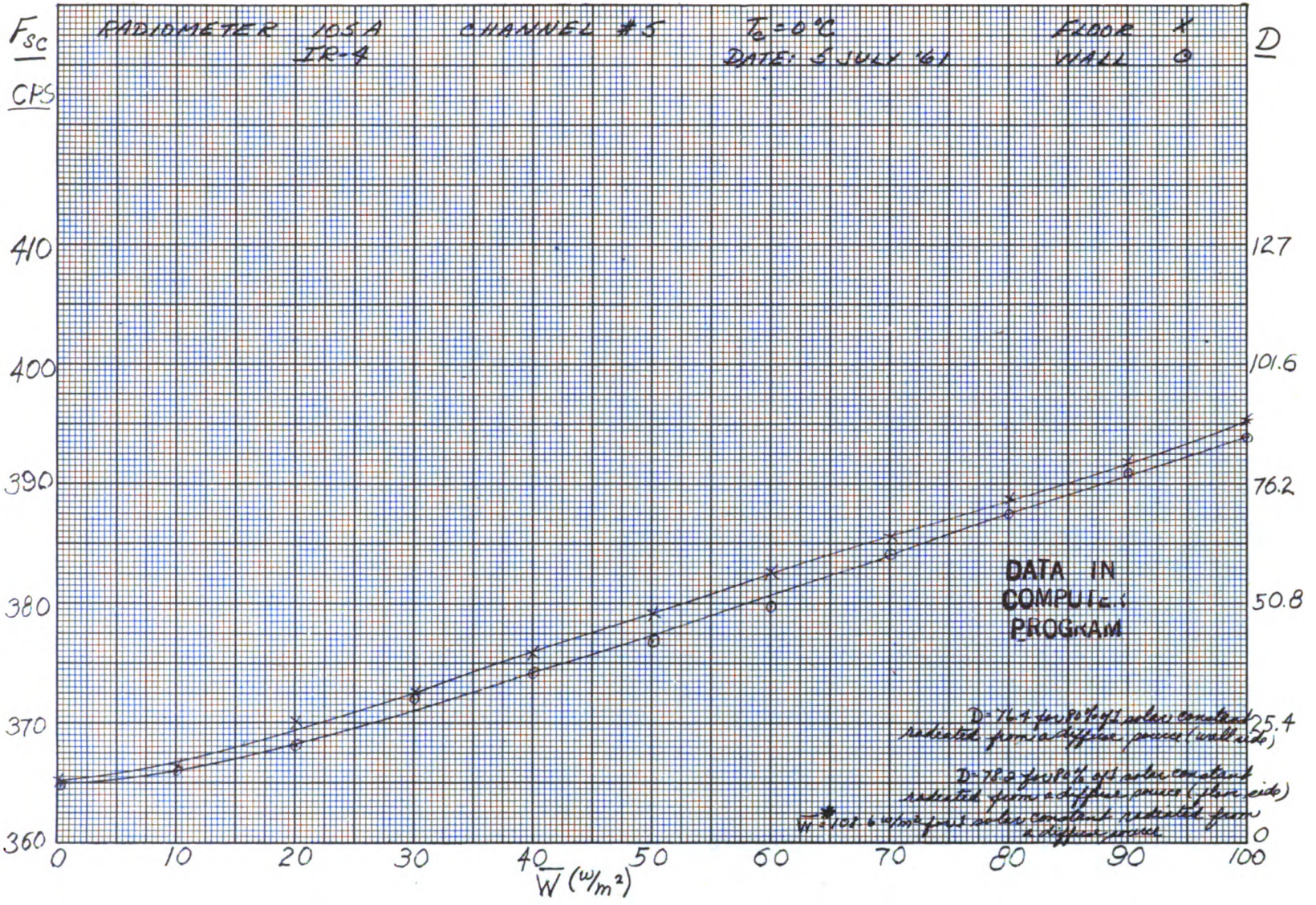

Figure 41—Subcarrier frequency and digital number vs. effective radiant emittance for wall and floor sides, Channel 5. (T_c = 0°C)

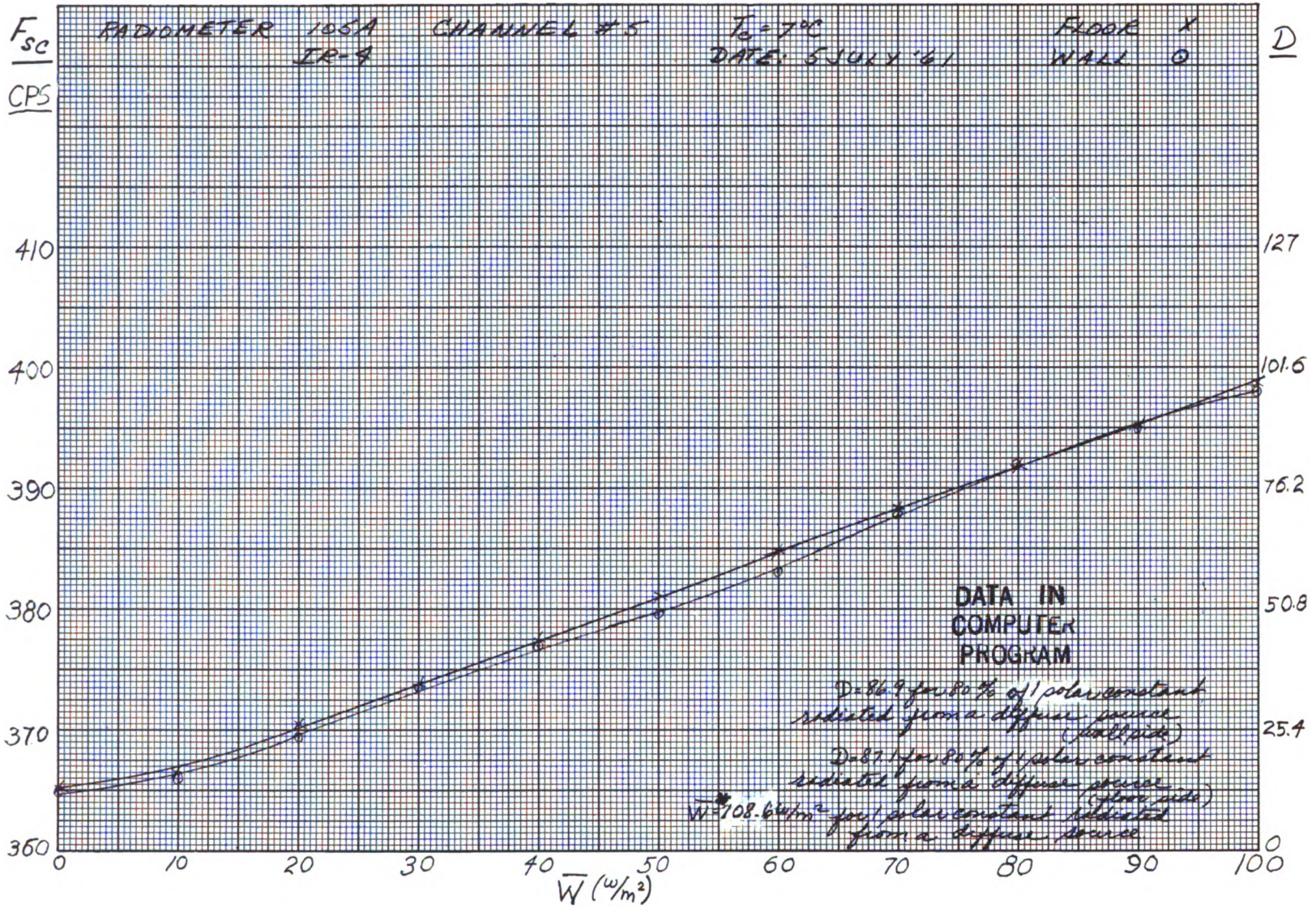

Figure 42—Subcarrier frequency and digital number vs. effective radiant emittance for wall and floor sides, Channel 5. (T_c = 7°C)

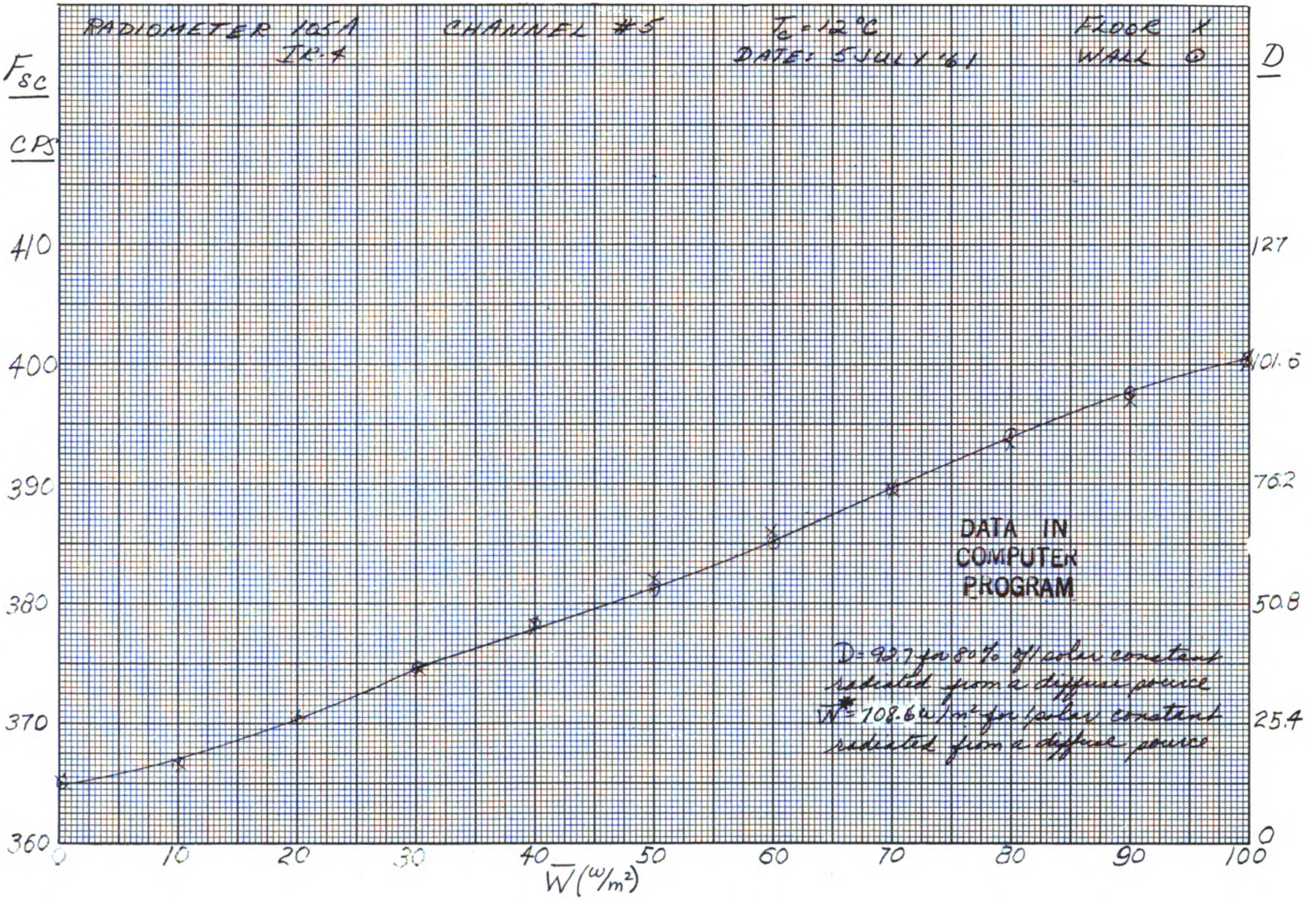

Figure 43—Subcarrier frequency and digital number vs. effective radiant emittance for wall and floor sides, Channel 5. (T_c = 12°C)

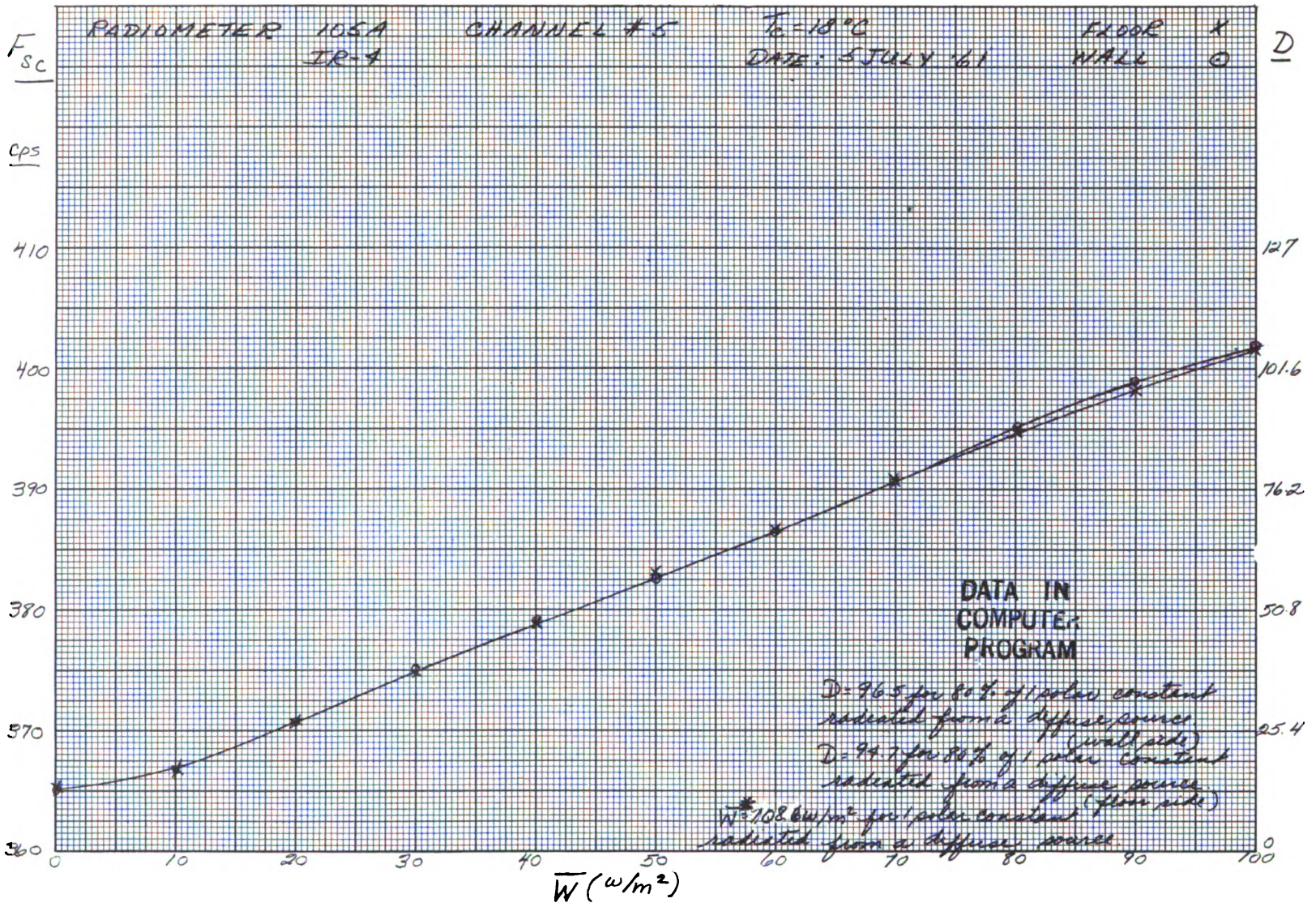

Figure 44—Subcarrier frequency and digital number vs. effective radiant emittance for wall and floor sides, Channel 5. (T_c = 18°C)

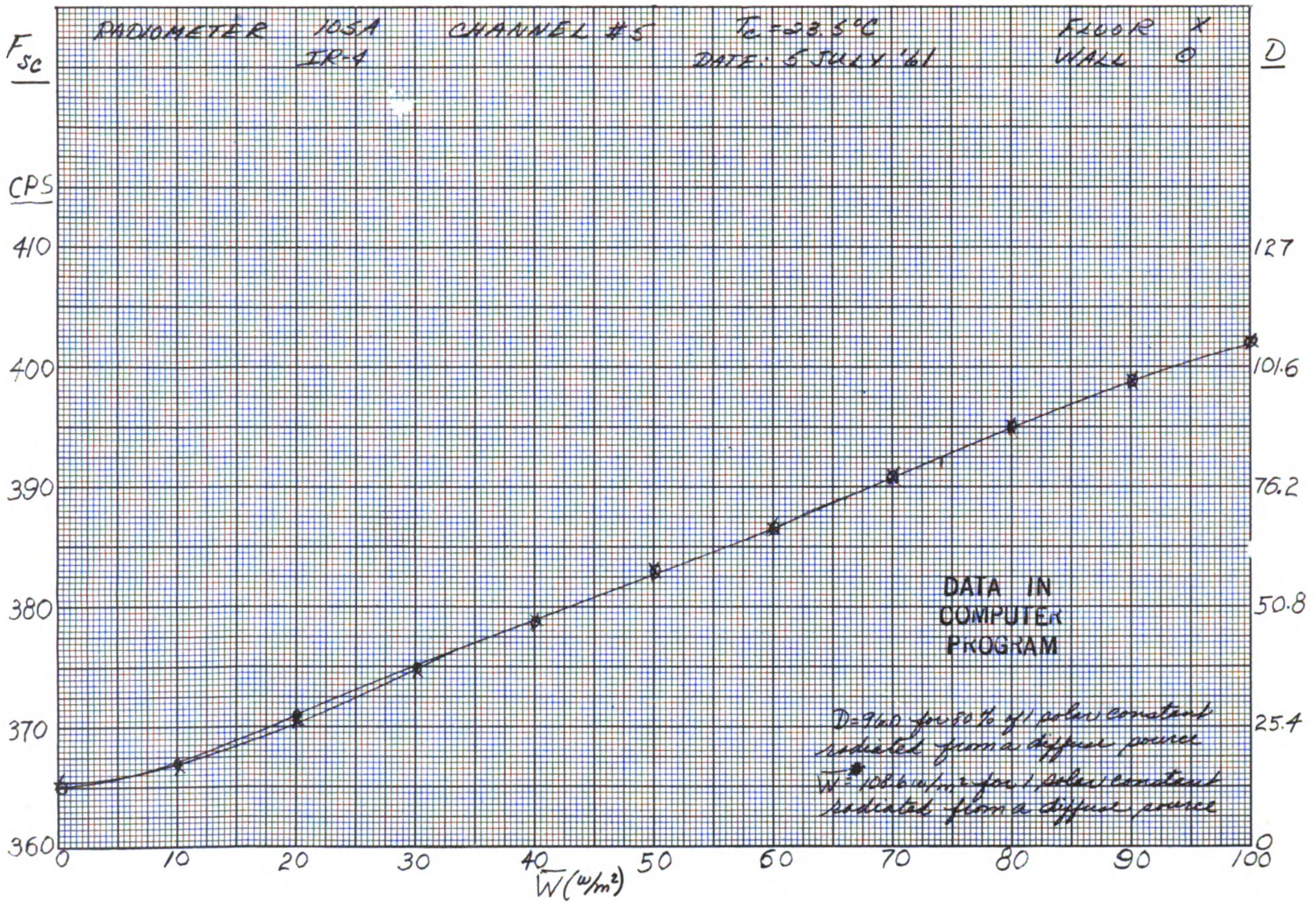

Figure 45—Subcarrier frequency and digital number vs. effective radiant emittance for wall and floor sides, Channel 5. (T_c = 23.5°C)

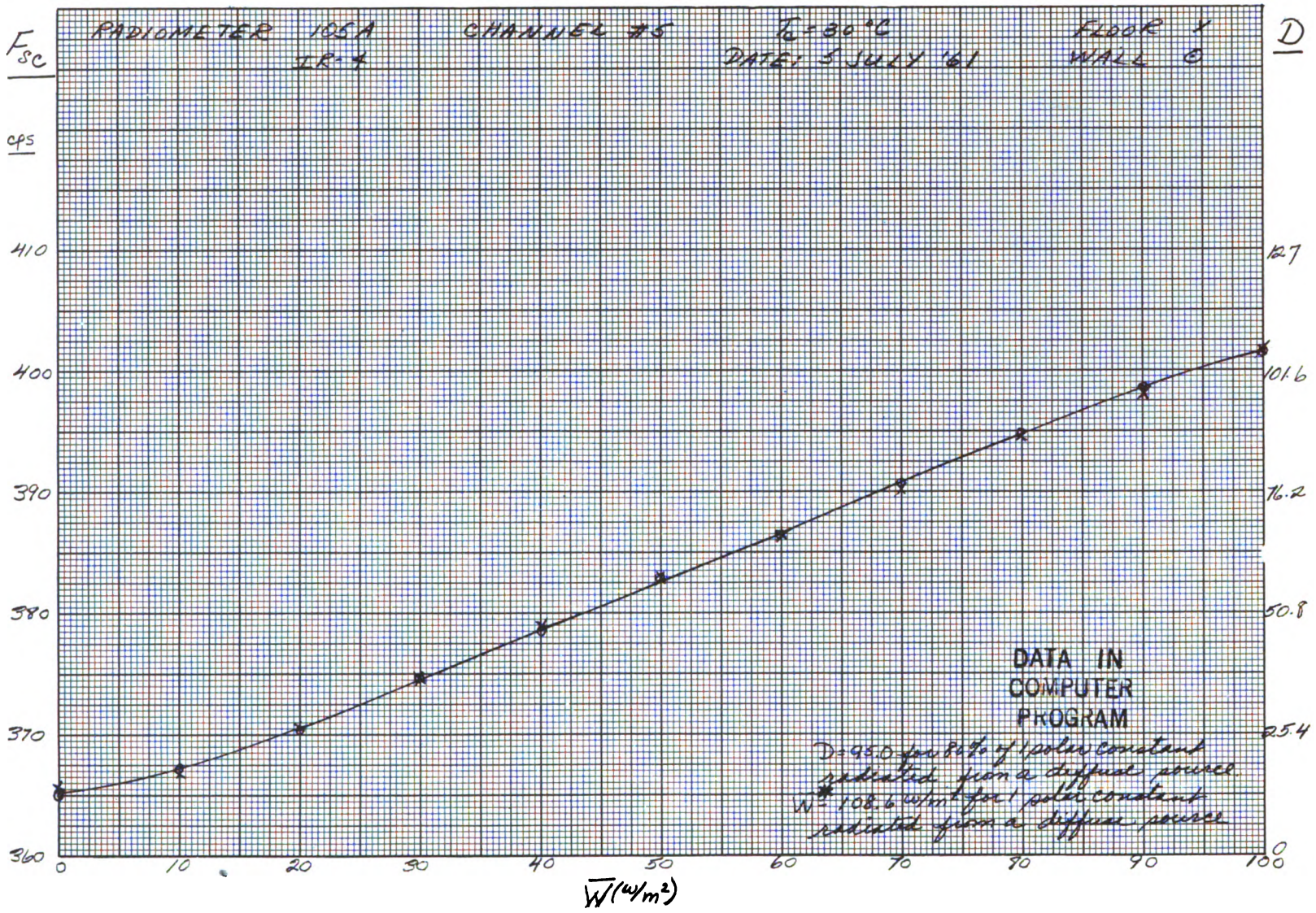

Figure 46—Subcarrier frequency and digital number vs. effective radiant emittance for wall and floor sides, Channel 5. (T_c = 30°C)

664272 O - 62 - 5

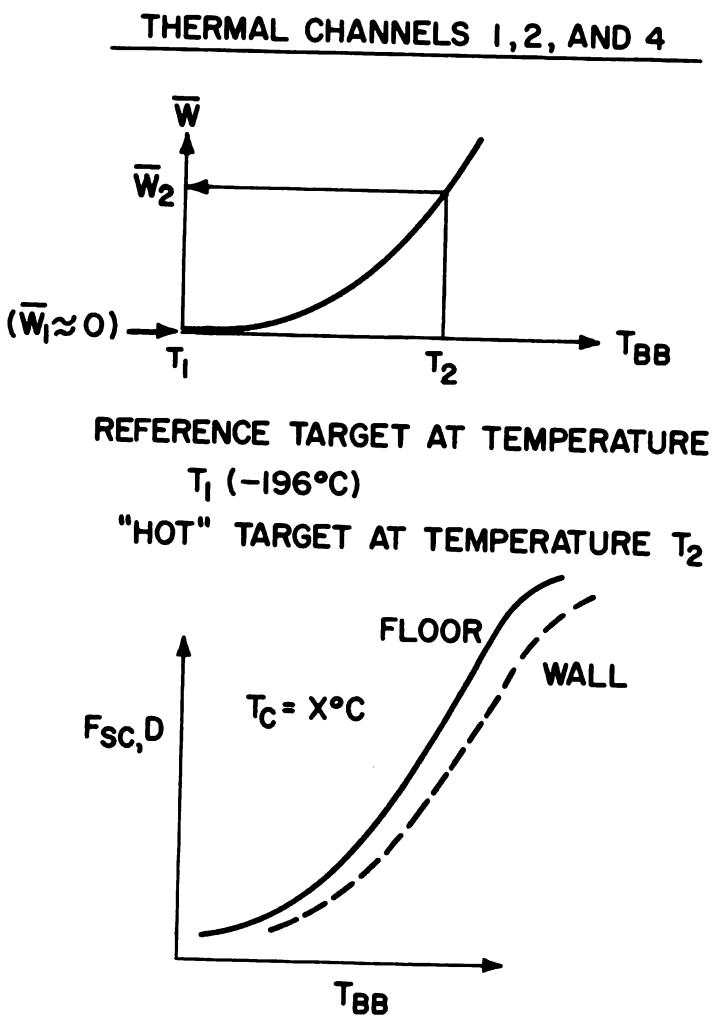

Figure 47—(a) Calibration of the thermal Channels 1, 2, and 4. (b) Calibration of the visible Channels 3 and 5.

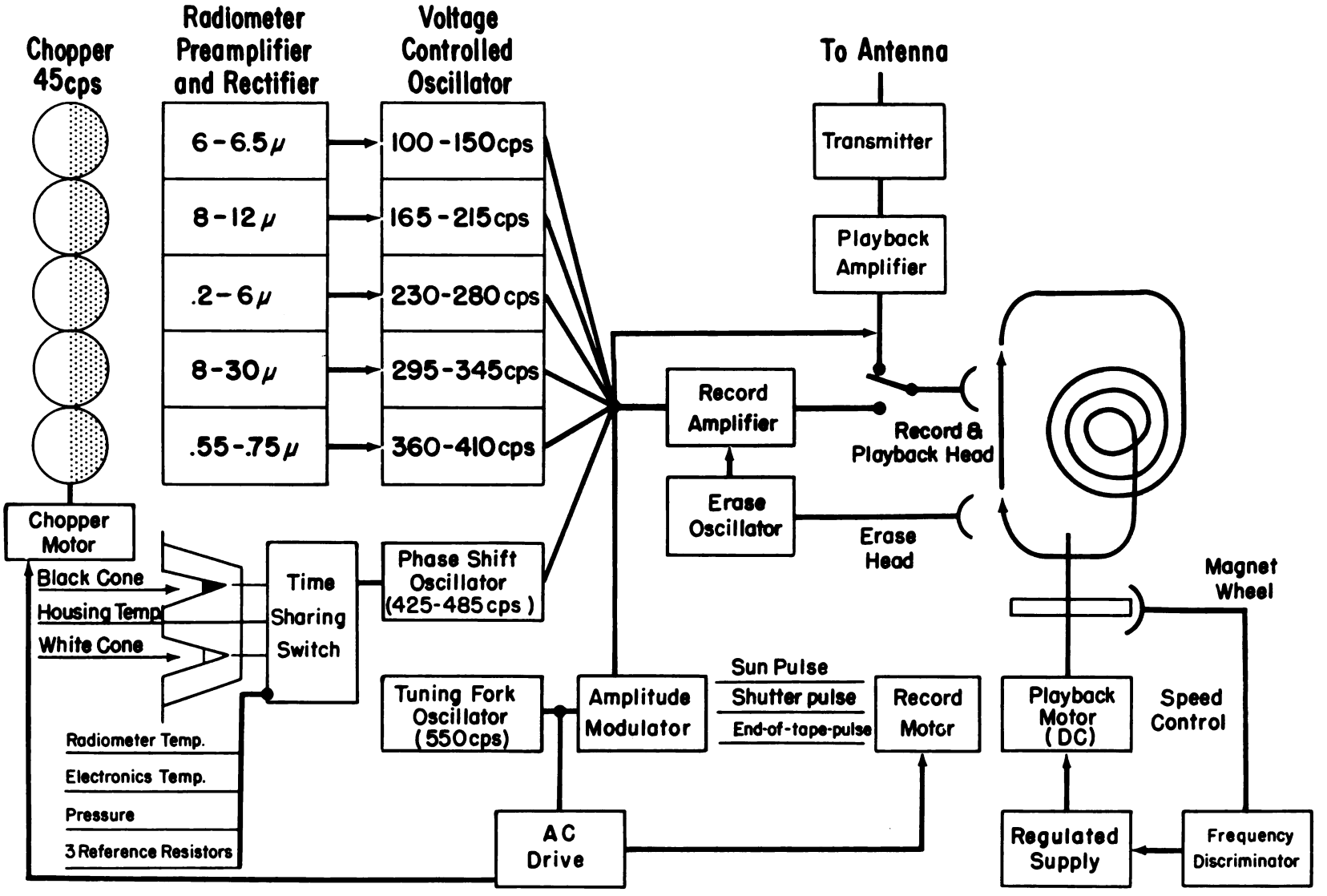

Figure 48—Block diagram of the radiation experiment in the satellite.

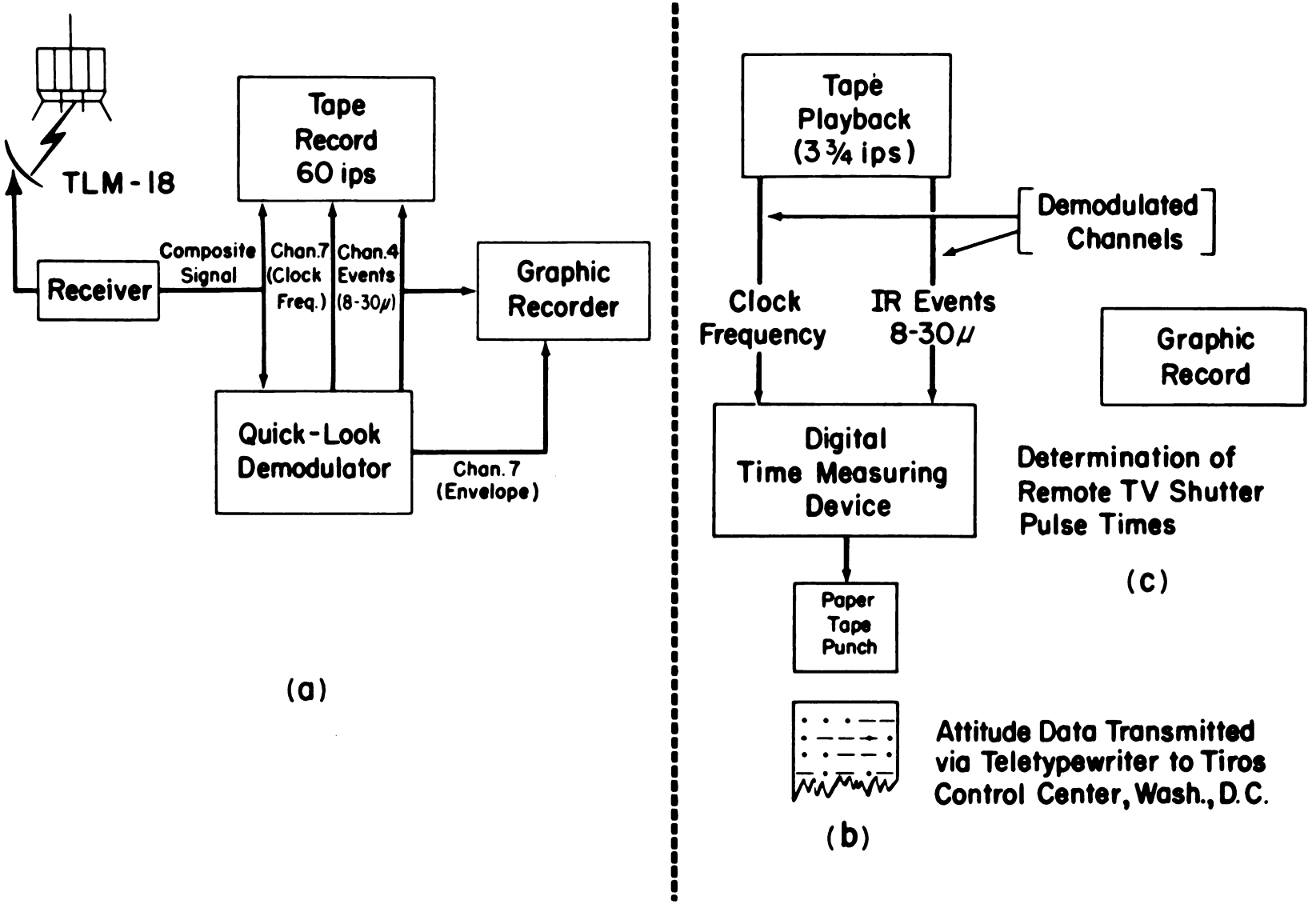

Figure 49—Block diagram of information flow at a data acquisition station including auxiliary uses of the radiation data.

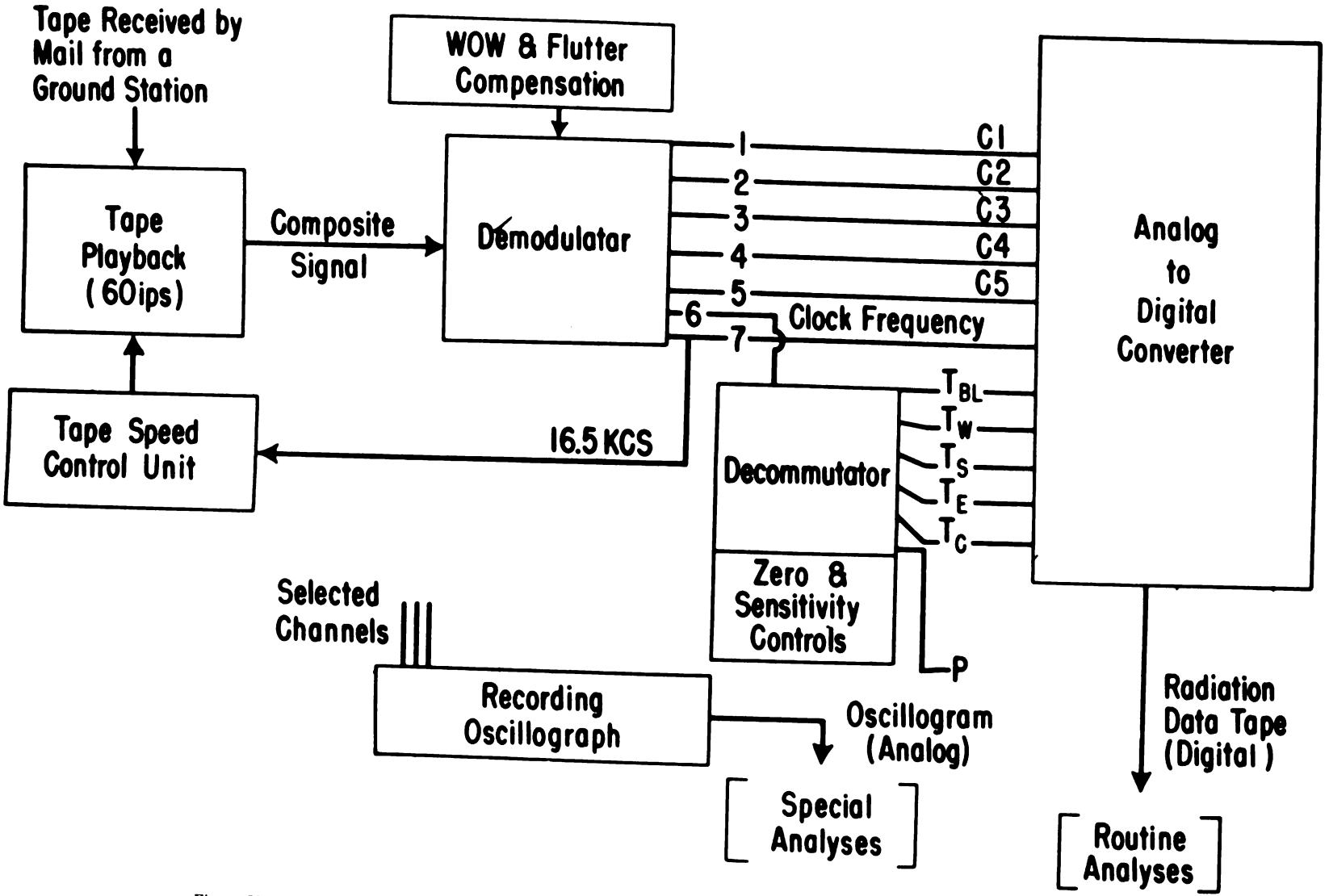

Figure 50—Block diagram of information flow at the data reduction center in producing a digital magnetic tape for computer input.

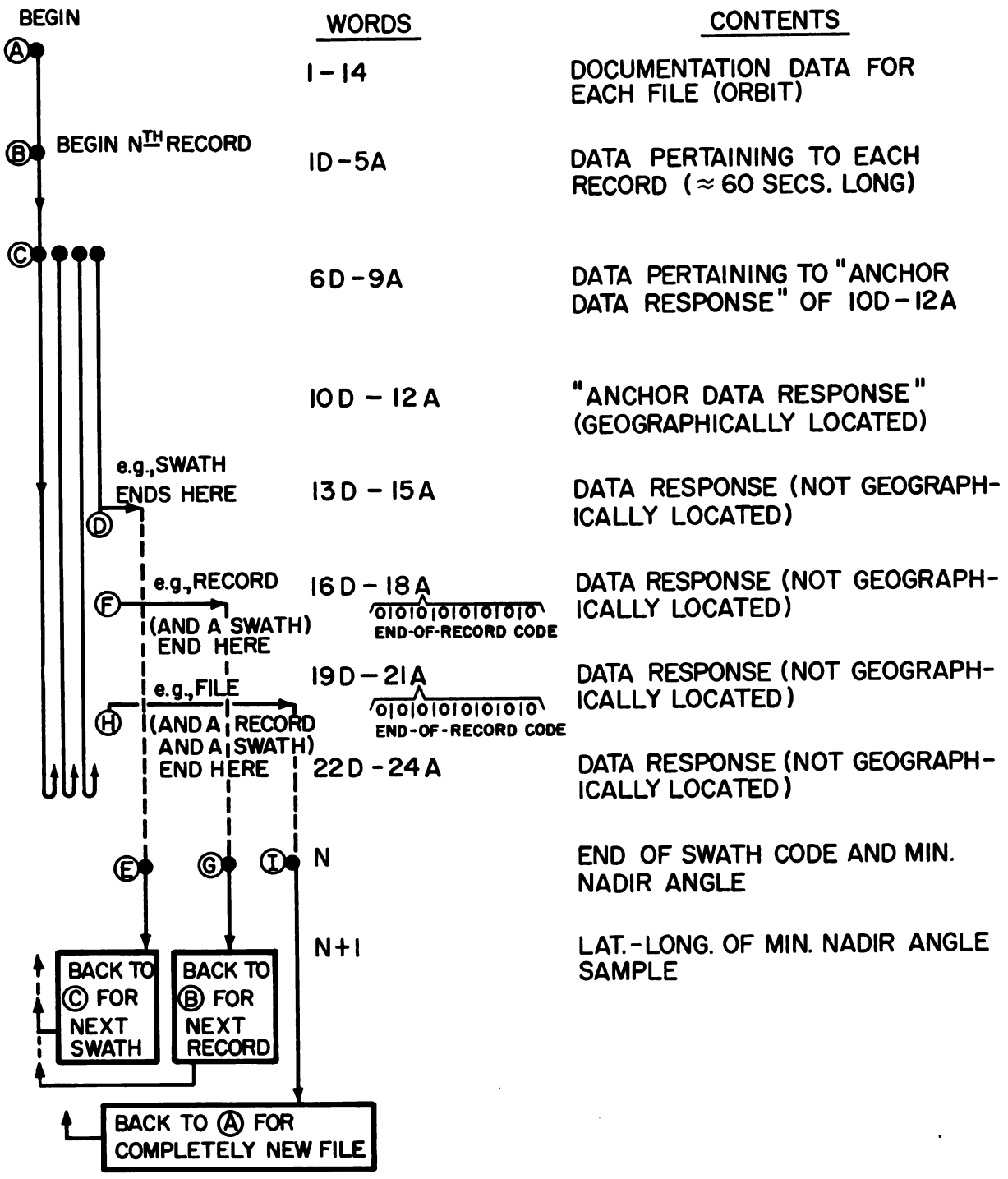

Figure 51—Diagram for interpretation of FMR tape format.

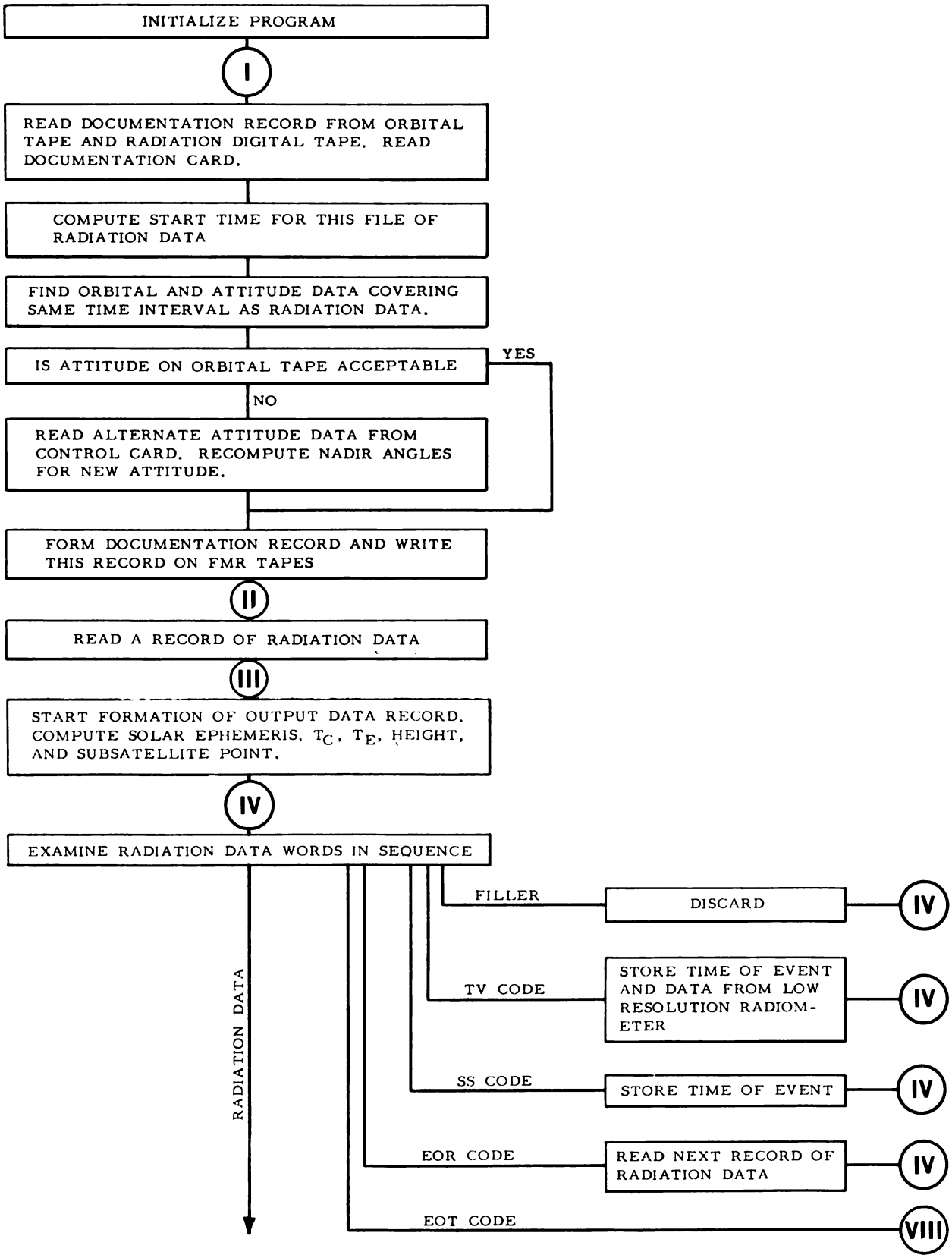

Figure 52—(a, b, c, & d)—Flow diagram for the IBM 7090 computer program used in reducing the radiation data.

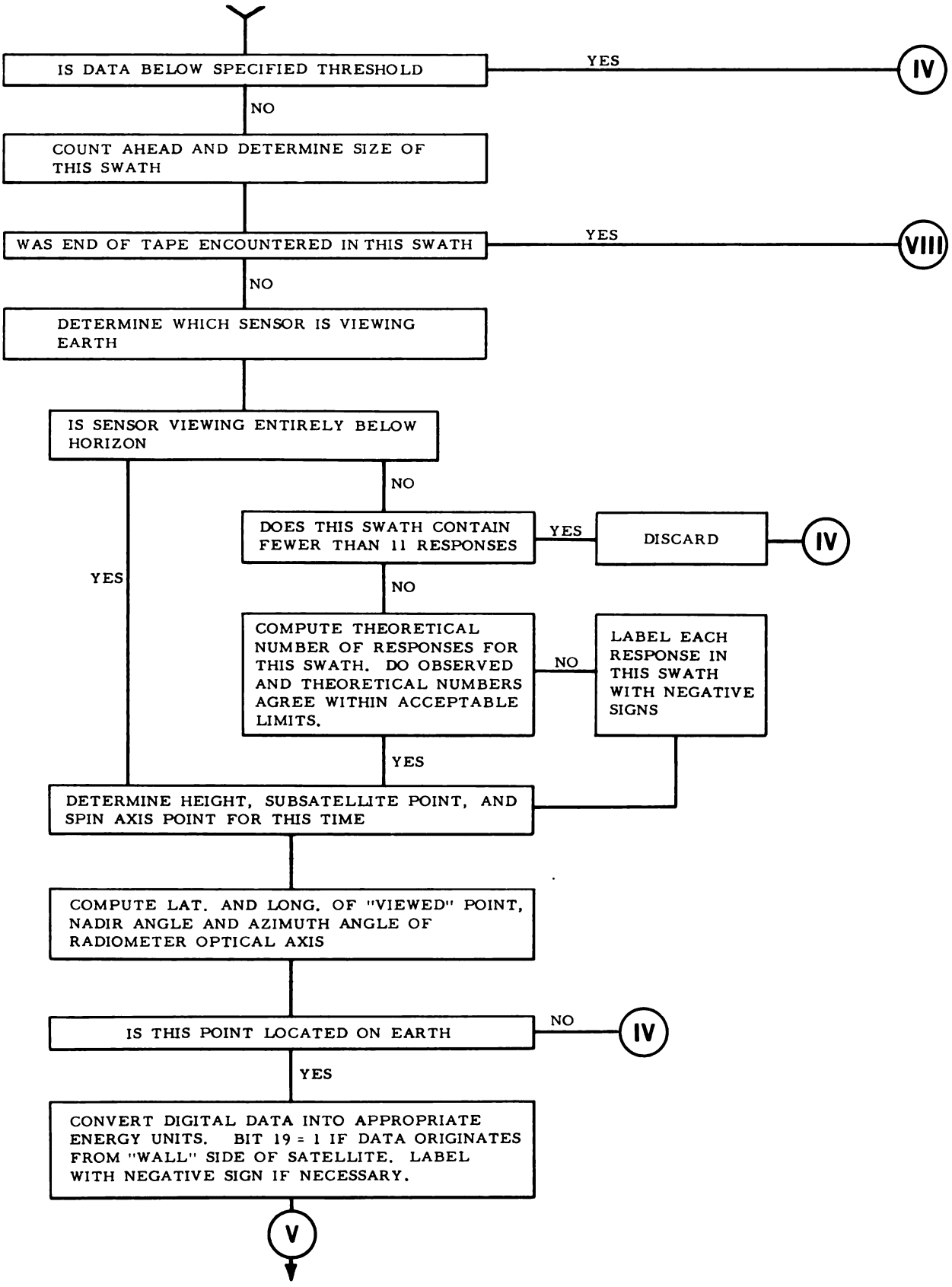

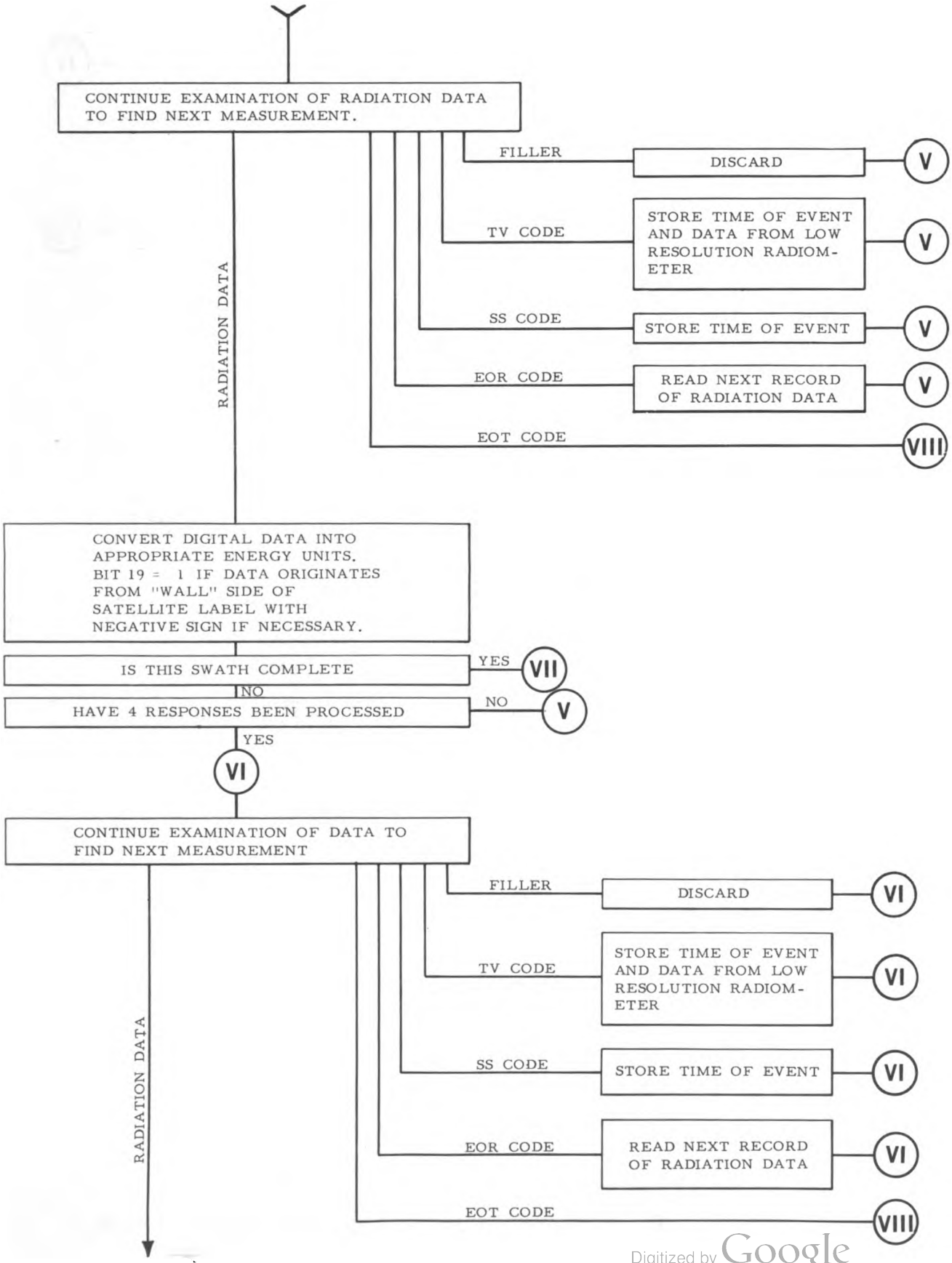

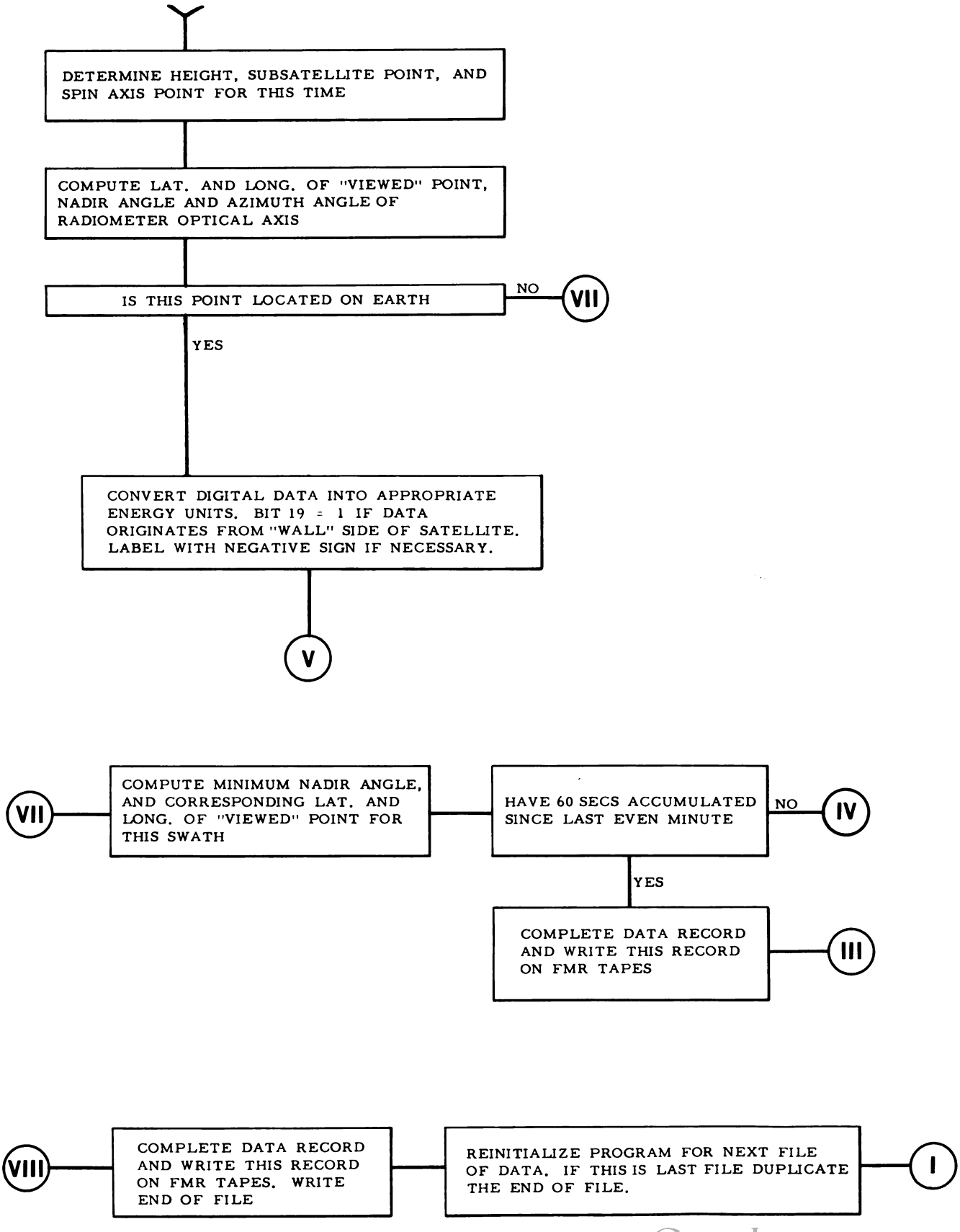

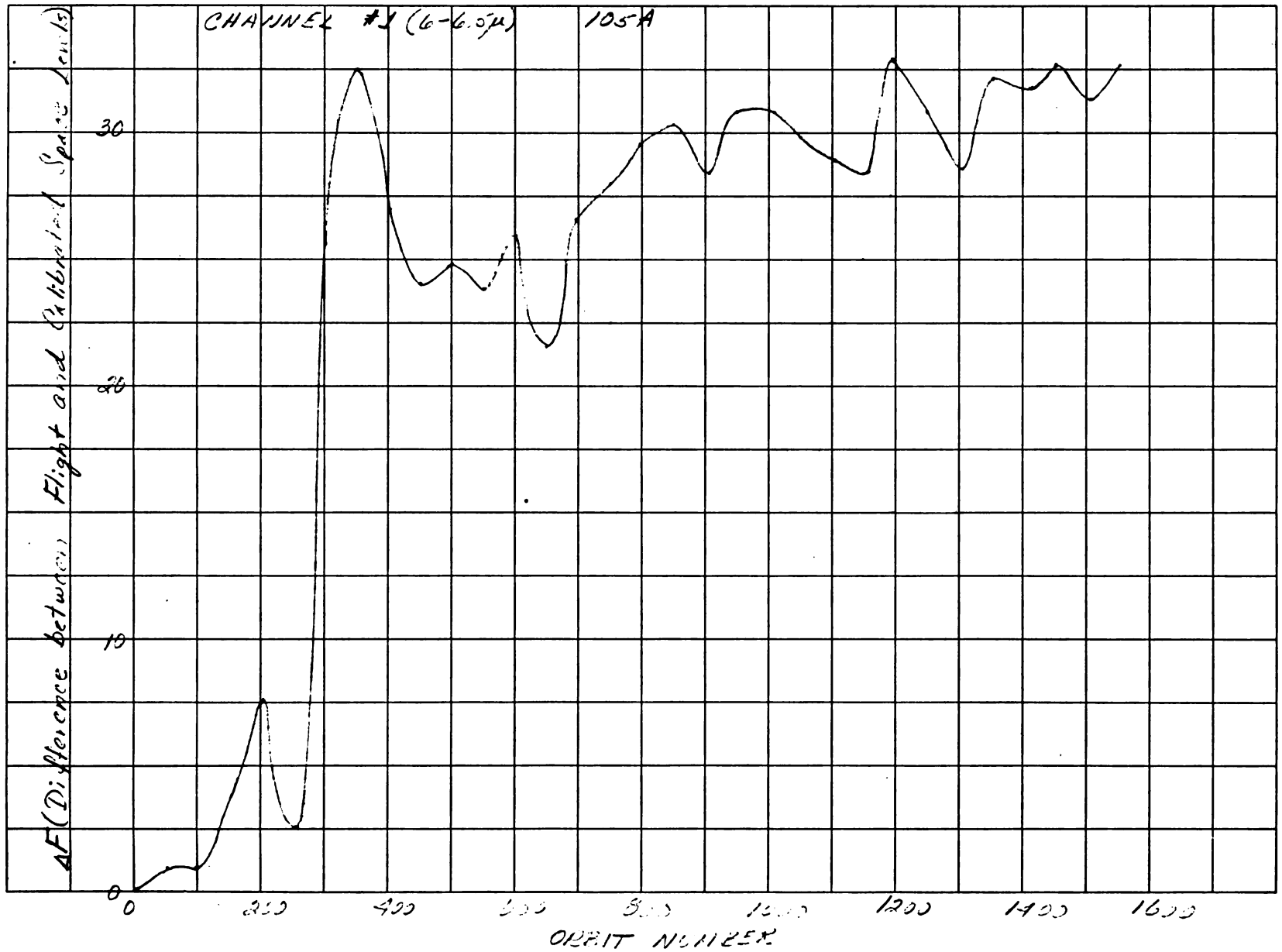

Figure 53—Difference between flight and calibrated space level vs. orbit number, Channel 1.

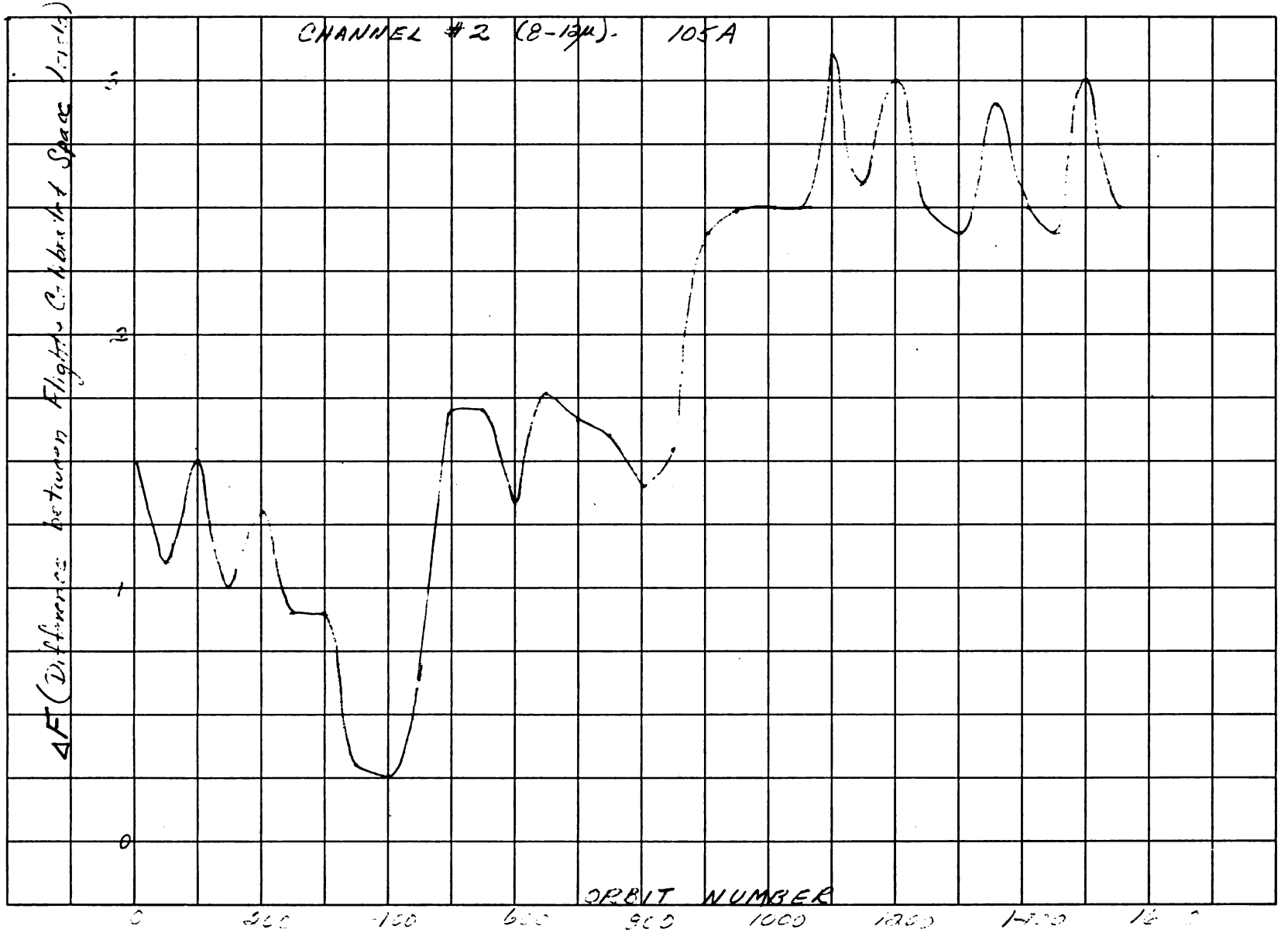

Figure 54—Difference between flight and calibrated space level vs. orbit number, Channel 2.

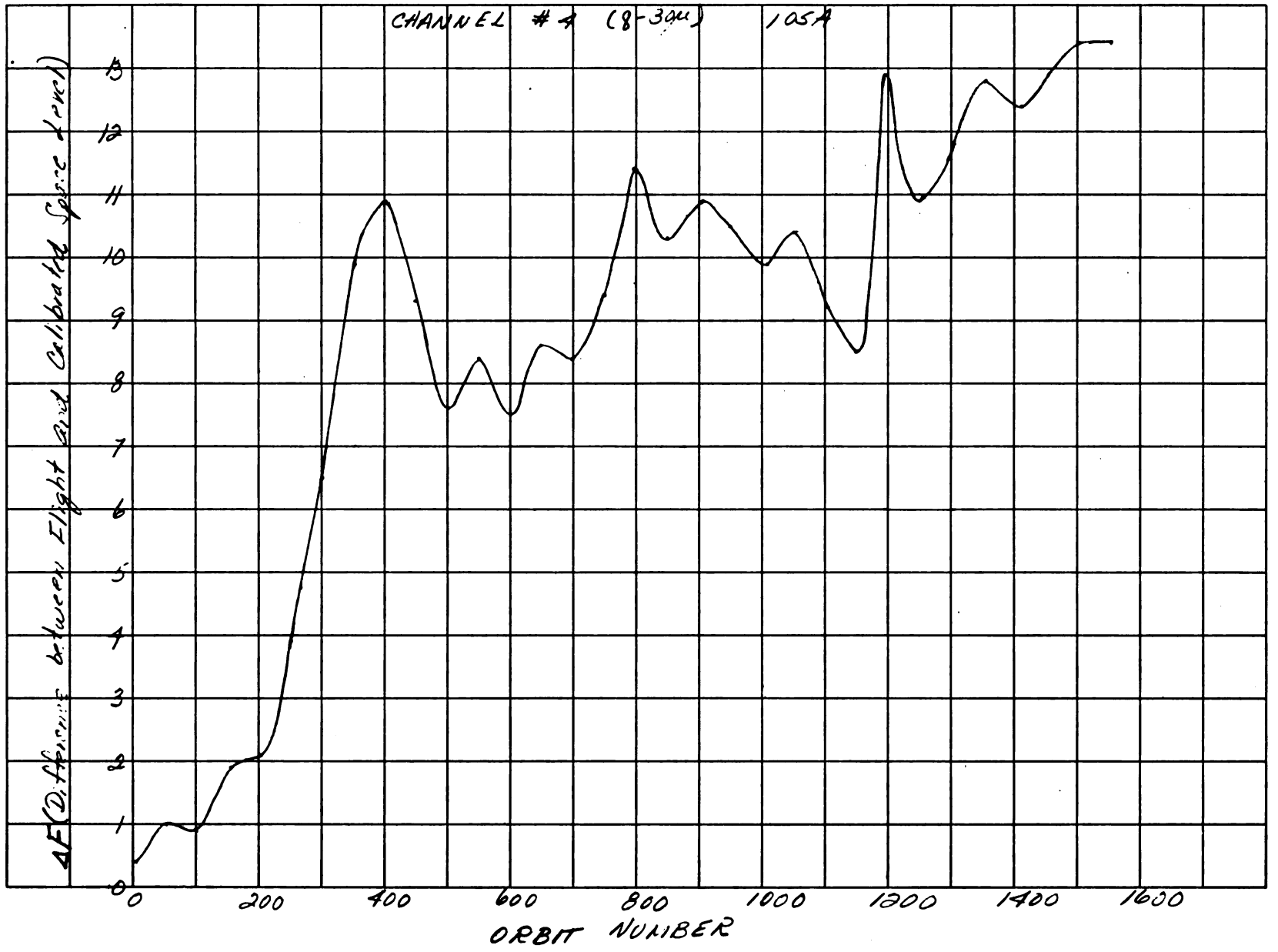

Figure 55—Difference between flight and calibrated space level vs. orbit number, Channel 4.

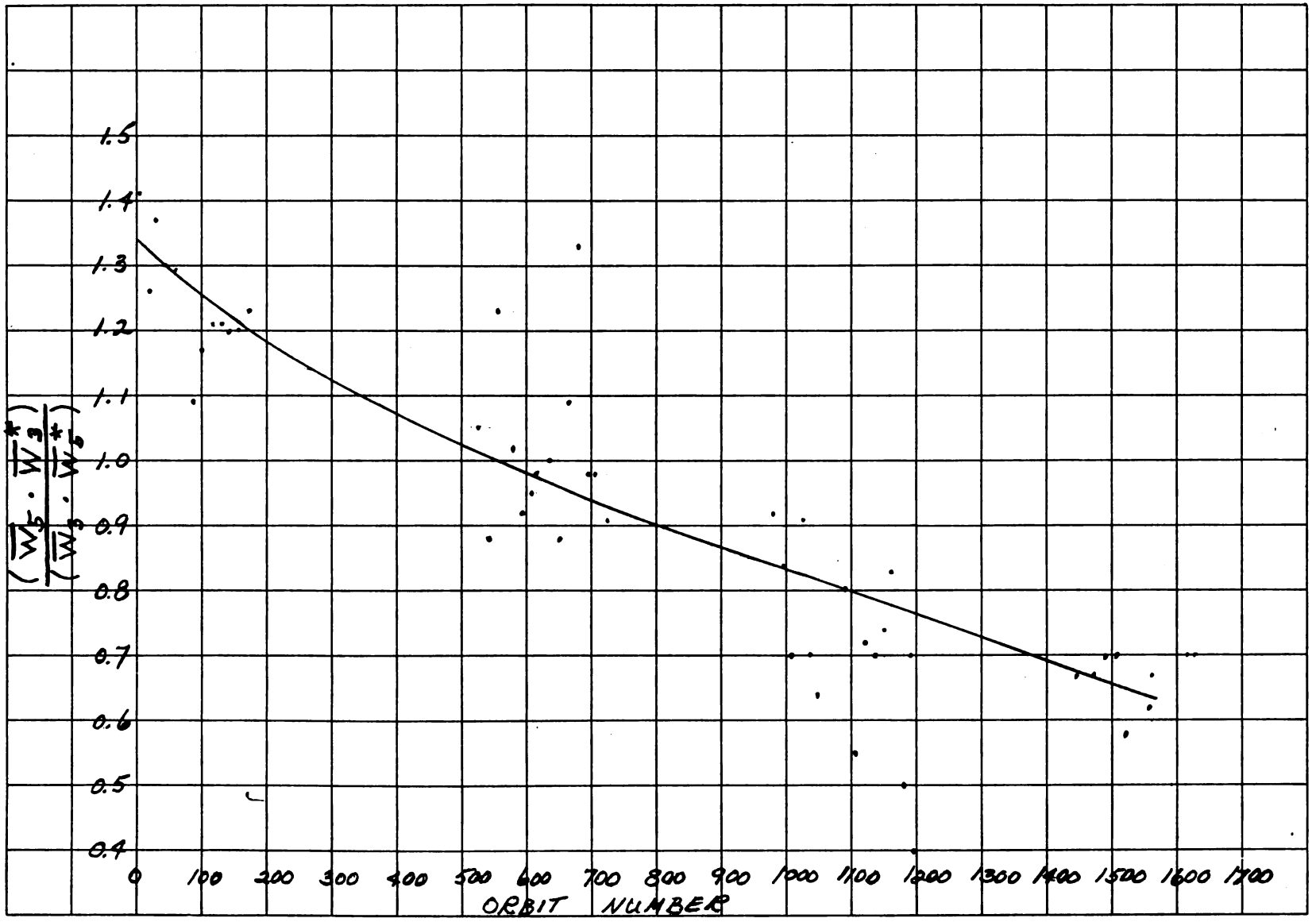

Figure 56—Ratio of $\overline{W}_6/\overline{W}_6^*$ to $\overline{W}_3/\overline{W}_3^*$ vs. orbit number.

DATE DUE

NOV 25 1964			
OCT 17 1965			
NOV 3 1965			
NOV 23 1965			